

## Three-nucleon force effects in cross section and spin observables of elastic deuteron-proton scattering at 90 MeV/nucleon

H. R. Amir-Ahmadi,<sup>1,\*</sup> R. Castelijns,<sup>1</sup> A. Deltuva,<sup>2</sup> M. Eslami-Kalantari,<sup>1</sup> E. D. van Garderen,<sup>1</sup> M. N. Harakeh,<sup>1</sup> N. Kalantar-Nayestanaki,<sup>1,†</sup> M. Kiš,<sup>1</sup> H. Löhner,<sup>1</sup> M. Mahjour-Shafiei,<sup>1</sup> H. Mardanpour,<sup>1</sup> J. G. Messchendorp,<sup>1</sup> B. Mukherjee,<sup>1</sup> D. Savran,<sup>1,3</sup> K. Sekiguchi,<sup>4</sup> S. V. Shende,<sup>1</sup> H. Witała,<sup>5</sup> and H. J. Wörtche<sup>1</sup>

<sup>1</sup>*Kernfysisch Versneller Instituut (KVI), University of Groningen, Zernikelaan 25, 9747 AA, Groningen, The Netherlands*

<sup>2</sup>*Centro de Fisica Nuclear da Universidade de Lisboa, Lisboa, Portugal*

<sup>3</sup>*Institut für Kernphysik, Technische Universität Darmstadt, Darmstadt, Germany*

<sup>4</sup>*RIKEN, Institute of Physical and Chemical Research, Wako, Saitama 351-0198, Japan*

<sup>5</sup>*Institute of Physics, Jagiellonian University, Cracow, Poland*

(Received 17 July 2006; published 6 April 2007)

The cross section and several spin-dependent observables have been measured with high precision for the reaction  $H(\vec{d}, \vec{p})d$  at 90 MeV/nucleon. Several calculations were performed based either purely on two-nucleon potentials or also including three-nucleon potentials (3NP). The cross sections are consistent with all calculations including 3NPs. However, no single calculation reproduces the analyzing powers and spin-transfer coefficients, although some spin observables are reproduced to various degrees by the different calculations. A good understanding of the spin structure of 3NP is still lacking.

DOI: [10.1103/PhysRevC.75.041001](https://doi.org/10.1103/PhysRevC.75.041001)

PACS number(s): 21.45.+v, 21.30.-x, 24.70.+s, 25.10.+s

The nucleon-nucleon ( $NN$ ) force has been studied extensively since the discovery of the neutron. Several two-nucleon potential (NNP) models have been developed over the decades and tested using nucleon-nucleon scattering data. Collecting over 4300 pp and  $np$  scattering data as is done for the Nijmegen data set [1] provides a good basis to develop high-quality NNPs, namely NijmI, NijmII [2], CD-Bonn (CDB) [3], and  $AV_{18}$  [4]. Also, a partial wave analysis (PWA) has been performed using the Nijmegen data set [5]. All the models and the PWA describe the phenomena involving only two nucleons with high accuracy. However, the NNPs are not very successful in describing various observables in three- or more-nucleon systems. For example, the binding energies of the light systems cannot be described at all by exact calculations that only use NNPs [6]. Also, in scattering problems such as elastic proton-deuteron scattering at intermediate energies, the exact calculations of the cross section, in which one only takes NNPs into account, underestimate the data in the minimum of the cross section [7,8].

At energies larger than 100 MeV/nucleon, the discrepancies are partially remedied by adding the necessary ingredients accounting for the potential (or the force) between the three nucleons (3NP). Similar conclusions, more or less, hold for spin observables [8–14]. However, none of the existing 3NP models accounts for all the existing data. Given the large number of possible 3NP structures, experiments involving three-nucleons will continue to play an essential role in our understanding of the nuclear potential.

The 3NP has been receiving more attention both theoretically and experimentally in the past years. Several 3NP models have been developed on the basis of the two-pion-exchange

mechanism, such as the Tucson-Melbourne (TM') [15,16], the Hanover [17], and the Urbana (UIX, IL2 and IL4) models [6,18]. In TM', a pion emitted from one nucleon is scattered by a second nucleon before being absorbed by the third nucleon. The Hanover model, CDB+ $\Delta$ , yields an effective 3NP by the explicit  $\Delta$ -isobar excitation, where the transition potential from  $NN$  to  $N\Delta$  state is based on  $\pi$  and  $\rho$  exchange. The UIX potential has been developed together with  $AV_{18}$  to fix the binding energy of light nuclei. It also includes  $s$ -wave and  $p$ -wave  $\pi N$  scattering.

The models mentioned above can be examined with scattering data. The scattering observables are predicted theoretically with any of the potential models using the Faddeev equations for the three-body scattering problem that can be solved exactly. The results of the scattering experiments also provide insight into the theoretical aspects of a model enabling one to improve the models further (see Ref. [19] in which the cross-section data lead to the conclusion that NNP is absolutely not sufficient to describe the data and only the inclusion of 3NP removes most of the deficiencies). There are a variety of observables that can be measured in a scattering experiment namely cross section and spin-dependent observables such as analyzing powers, induced polarization, and spin-transfer coefficients (STC) [20]. Presently, only a few data sets are available for nucleon-deuteron elastic scattering at intermediate energies between 70 to 200 MeV. Cross sections and analyzing powers for the  ${}^2H(\vec{p}, p)d$  reaction at 108, 120, 135, 150, 170, and 190 MeV have been measured at KVI [7–10]. The reaction  $H(\vec{d}, \vec{p})d$  was studied at RIKEN at 70, 100, and 135 MeV/nucleon [11–14]. At RCNP, the nucleon-deuteron reaction was studied at 250 MeV [21,22]. The only measurement of spin-correlation coefficients up to now was performed at IUCF at 135 and 200 MeV [23–25]. In the present work which was performed at KVI, we present the results of the cross sections, the analyzing powers, the induced polarizations and the STCs measured for the reaction

\*Electronic address: amirahmadi@kvi.nl

†Electronic address: nasser@kvi.nl

$H(\vec{d}, \vec{p})d$  at 90 MeV/nucleon. This energy was chosen because of the possibility of being able to compare the results of the various theoretical models, including the emerging results of chiral perturbation theories at intermediate energies [26,27], with the experimental results. These theories which generate nuclear many-body potentials are, presently, reliable only at lower energies.

The present experiment was performed using the Big-Bite Spectrometer (BBS) [28] and the proton polarimeter of the EuroSuperNova (ESN) collaboration [29]. The detector setup of the experiment is extensively discussed in Ref. [29]. Polarized deuterons for which the polarization was switched between five states labeled as Off,  $(p_z, p_{zz}) = (0, 0)$ , positive vector,  $(2/3, 0)$ , negative vector,  $(-2/3, 0)$ , positive tensor,  $(0, 1)$ , and negative tensor,  $(0, -2)$  were produced by the KVI polarized-ion source (POLIS). After accelerating the deuterons to 180 MeV by the AGOR cyclotron, the polarization of the deuterons was measured continuously during the whole experiment by the In-Beam Polarimeter [30]. The beam polarization was obtained by measuring the elastic scattering of deuterons from a proton target at a fixed angle of  $100^\circ$  with this polarimeter, and subsequently comparing the measured asymmetries with the interpolated analyzing power of the same reaction at the same angle but at various energies recently compiled in Ref. [31]. The measured polarizations were typically 50–60% of the theoretical values mentioned above with small admixtures of the components which should be theoretically zero. The polarized deuterons then impinged on a hydrogen target in the target chamber of BBS. Depending on the reaction rate, either a solid  $\text{CH}_2$  foil or a liquid hydrogen target was used. The strength of the dipole magnet of BBS was set so that the scattered protons from the reaction  $H(\vec{d}, \vec{p})d$  were focused in the middle of the focal-plane of the dipole magnet. There are two vertical-drift chambers (VDC) at the focal-plane with which the track of particles can be reconstructed. The polarization of the scattered protons was measured by the proton polarimeter ESN. The polarimeter uses a graphite slab as secondary target for the polarization measurement. The track of the protons after scattering from the graphite slab was reconstructed with multiwire proportional chambers (MWPC) [32]. Knowing the track of the particles after the secondary scattering, one can obtain the asymmetry,  $A_s$ , of the  $p$ -C reaction for a given secondary scattering angle. This asymmetry is related to the polarization,  $p_y$ , of the incoming protons and the analyzing power,  $A$ , of the  $p$ -C reaction,  $A_s = Ap_y$ . The inclusive analyzing powers of  $p$ -C for the energy range of interest were measured in a separate calibration experiment [33].

For a polarization measurement, one must correct for the instrumental asymmetry of the polarimeter, even though it is very small. We measured the instrumental asymmetry of ESN polarimeter during the calibration experiment, which was done at a different time, to be about 0.02 using unpolarized protons. This measured instrumental asymmetry resulted in the induced polarizations for the reaction  $H(\vec{d}, \vec{p})d$  which were about 0.1 below the theoretical values. It is known that the induced polarization of the  $H(d, \vec{p})d$  reaction, apart from a minus sign, is equal to the analyzing power of the

time-reversed reaction of  ${}^2\text{H}(\vec{p}, d)p$ . This analyzing power was systematically studied at KVI [8,10]. The results of the analyzing powers were well described by  $\text{CDB} + \Delta$  calculations around the energy of interest. Therefore, it was decided to determine the instrumental asymmetry as a free parameter in a fit of the data to  $\text{CDB} + \Delta$  calculations. Thus for this observable, only the shape of the distribution is relevant.

In this Rapid Communication, the results of measurements for the cross sections,  $d\sigma/d\Omega$ , the vector analyzing powers,  $A_y$ , the tensor analyzing powers,  $A_{yy}$ , the induced polarizations,  $P_{y'}$ , the vector STCs,  $K_{y'}$ , and the tensor STCs,  $K_{yy'}$  are presented. The measurements were performed in the angular range of  $90^\circ$ – $170^\circ$  in the center-of-mass (c.m.) frame. The relations between the observables are given by:

$$I(\theta) = I_0(\theta) \left[ 1 + \frac{3}{2} p_y A_y(\theta) + \frac{1}{2} p_{yy} A_{yy}(\theta) \right],$$

$$p_{y'} I(\theta) = I_0(\theta) \left[ P_{y'}(\theta) + \frac{3}{2} p_y K_{y'}(\theta) + \frac{1}{2} p_{yy} K_{yy'}(\theta) \right],$$

where  $I$  is the spin-dependent cross section,  $I_0 \equiv d\sigma/d\Omega$  is the unpolarized cross section,  $p_{y'}$  is the polarization of the protons after the primary scattering, and  $p_y(p_{yy})$  is the vector(tensor) polarization of the incoming deuterons. The experimental results along with the calculations are shown in Fig. 1. The error bars, which are included for each data point, are for some data points smaller than the symbol size of the point. This error accounts for the statistical uncertainties and a very small point-to-point (PTP) uncertainty. The statistical uncertainties come from the spin-dependent cross sections and the statistical uncertainty in determining the incoming-beam polarization. The small PTP uncertainty accounts for a small instability of the experimental apparatus over long periods of time and background subtraction. These errors are still very small, which shows an acceptable stability of the detector. The PTP uncertainty at  $170^\circ$  is larger than at the other points. For this point, the Faraday cup had to be placed inside the dipole magnet of BBS. In this case, the incoming beam is deflected by the dipole magnet and so the Faraday cup must be positioned very precisely. Therefore, small movements of the beam spot or changing the magnet strength can have a magnified effect on the error. Other systematic uncertainties originate from the target thickness measurement, the estimation of the angular opening of the detector, the total collected charge in the Faraday cup, and the systematic error of the incoming beam polarization. The resultant systematic error is  $\sim 5\%$  for the cross sections and  $\lesssim 3\%$  for all other spin-dependent observables.

The calculations based on various NNPs are slightly different, and because none of them is a priori preferred, the spread of the theoretical predictions can be considered as the theoretical uncertainty. Therefore, the calculations with different NNPs are shown by bands (dark gray), and those based on  $NN + \text{TM}'$  are shown as light gray bands. The result of a calculation with  $\text{AV}_{18} + \text{UIX}$  [6] is shown by a dashed line. All these calculations were performed by the Bochum-Cracow group [34]. The results of the calculations done by the Lisbon-Hanover group ( $\text{CDB} + \Delta$ ) are shown by solid lines. It is the only calculation that includes the Coulomb interaction between the protons [35]. The effect of

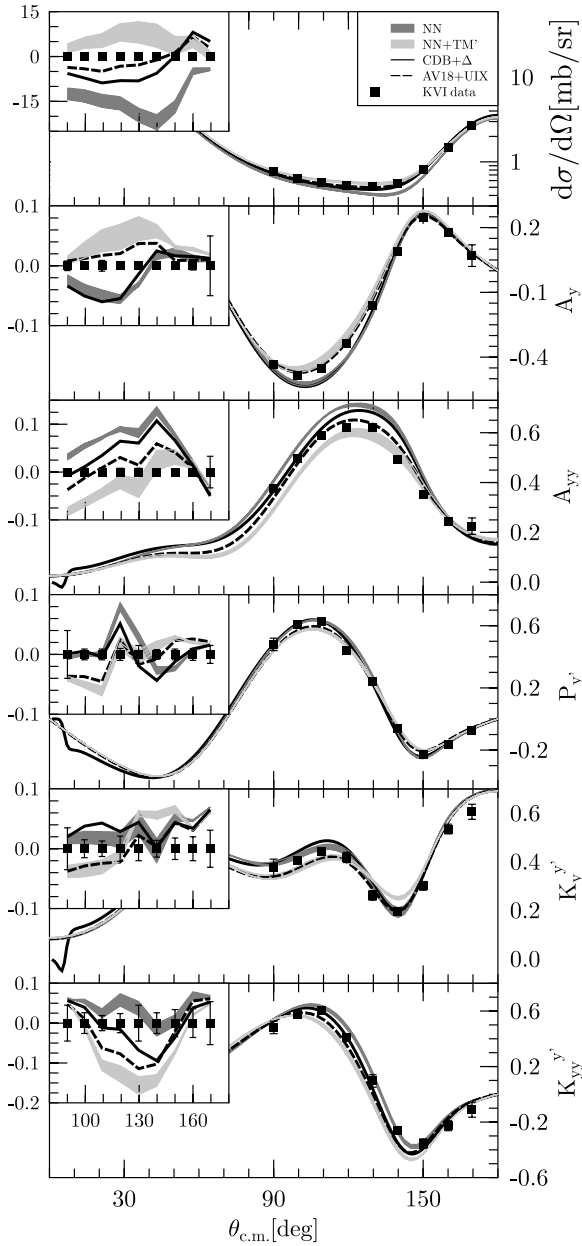


FIG. 1. The data for the cross sections,  $d\sigma/d\Omega$ , the vector,  $A_y$ , and tensor,  $A_{yy}$ , analyzing powers, the induced polarizations,  $P_{y'}$ , and the vector,  $K_{y'}$ , and tensor,  $K_{yy'}$ , STCs. Theoretical predictions based on NNP alone are shown by the dark gray bands, whereas those with  $NN+TM'$  are presented by the light gray bands. Dashed (solid) lines show the predictions using  $AV_{18}+UIX$ ( $CDB+\Delta$ ). For  $A_y$ , the solid line is on the lower edge of the dark gray band. The inset for each panel shows the percentage of (absolute) differences for the cross section (spin observables) measurements with the data points set to zero. The systematic uncertainty of 5% for the cross sections and 3% for the spin observables is not shown in the figure.

the Coulomb force is shown to be large for most observables of the elastic scattering only at small scattering angles.

The measured cross sections along with calculations are shown in the top panel of Fig. 1. The NNP band fails to describe the magnitude and the shape of the cross sections around the minimum. As expected for this energy, adding the

3NPs accounts for the differences. Taking the systematic error of the experiment into account, the measured cross sections are consistent with the results of all calculations including 3NP. To distinguish among the 3NP models, one should improve the systematic precision of the measurements drastically. The results show that the 3NPs are adequately understood as far as the spin-averaged cross sections at this energy is concerned.

The data points for the vector-analyzing power (Fig. 1, second panel from top) from  $90^\circ$  up to  $130^\circ$  are just in between the NNP band and  $NN+TM'$  band in the minimum of the analyzing power. The  $AV_{18}+UIX$  calculation slightly overestimates the data and the  $CDB+\Delta$  calculation underestimates them in the region of the minimum. Note that between  $50^\circ$  and  $120^\circ$  the  $CDB+\Delta$  calculation is at the lower limit of the NNP calculations and above  $120^\circ$  it is hidden in the NNP band. Above  $140^\circ$ , the two bands merge and are in agreement with the data. The closest calculation to this observable is  $AV_{18}+UIX$ . Also note that, in the band of  $NN+TM'$ , the calculation of  $AV_{18}+TM'$  is at the far edge from data and  $CDB+TM'$  is at the near edge. The data points for the tensor-analyzing power (Fig. 1, third panel from top) are well below the NNP band between  $100^\circ$  and  $150^\circ$ . The results do not seem to be fully described by any of the calculations, except may be by  $AV_{18}+UIX$ . The peak widths of the calculations are different and also different from the data. Because of this behavior, there is no trend in the agreement between the data and the calculations. At large and small angles, the NNP calculations are closer, whereas in the intermediate region, the 3NP calculations come closer to the data. In general, the  $AV_{18}+UIX$  3NP describes both analyzing powers better.

As was said before, the induced polarization (shown in the fourth panel from top of Fig. 1) was used to obtain the instrumental asymmetry of the polarimeter and as such is normalized to a calculation using one free parameter representing this asymmetry. Therefore, one may use only the shape of the angular distribution for this observable, which clearly follows the shape of all calculations relatively well.

The data points for the vector STCs (Fig. 1, second panel from bottom) follow the results of the NNP calculations most closely. The  $CDB+\Delta$  calculation (for most angles) also fit the data well. Obviously, the results of  $AV_{18}+UIX$  and  $NN+TM'$  cannot describe this observable as their shapes are also different from the data. The data points for the tensor STCs (Fig. 1, bottom panel) are in good agreement with the NNP band and in reasonable agreement with the results of the  $CDB+\Delta$  calculations. The data points from  $110^\circ$  to  $150^\circ$  are underestimated by  $NN+TM'$  calculations. In general, the calculations including the  $\Delta$ -dynamics show that the effect of the 3NP is small for the STCs. This is also confirmed by our measurement, in contrast to the results of the only other measurement of these observables at a higher energy of 135 MeV/nucleon [12].

If one normalizes the induced polarization to  $AV_{18}+UIX$  calculation rather than  $CDB+\Delta$ , the data points for  $120^\circ$  and larger do not change significantly for both the vector and tensor STCs. Only the values of the data at  $90^\circ$ ,  $100^\circ$ , and  $110^\circ$  become systematically smaller but well within the errors.

H. R. AMIR-AHMADI *et al.*

PHYSICAL REVIEW C **75**, 041001(R) (2007)

The vector STCs will then be closer to the NN+TM' band in that region.

In summary, cross sections, vector and tensor analyzing powers, induced polarizations, and vector and tensor spin-transfer coefficients have been measured with high precision for the reaction  $H(\vec{d}, \vec{p})d$  at 90 MeV/nucleon. The data were compared with theoretical predictions based on NNP and NNP+3NP. The cross section results clearly show the need to include 3NP in the calculations. The spin part of various 3NPs, however, reveals surprising features. There is no single 3NP which can describe all the spin observables. In general, the calculations based on AV<sub>18</sub>+UIX perform better for analyzing powers while the measured STCs are closer to 3NP predictions of CDB+ $\Delta$  which, in turn, are very close to the results based

on NNP only. These features need to be better understood in theory.

The authors acknowledge the efforts of the AGOR and the ion source groups at KVI in providing the high-quality beams needed for these measurements. We thank A. M. van den Berg and M. Hunyadi for their help in running the BBS/ESN detector. This work was performed as part of the research program of the Stichting voor Fundamenteel Onderzoek der Materie (FOM) with financial support from the Nederlandse Organisatie voor Wetenschappelijk Onderzoek (NWO) and by the Polish Committee for scientific research under grant no. 2p03B00825. The numerical calculations have been performed on the IBM Regatta p690+ on the NIC in Jülich, Germany.

- 
- [1] Online-Calculation from Nijmegen Potentials and Partial-Wave Analysis, [www.nn-online.sci.kun.nl](http://www.nn-online.sci.kun.nl)
- [2] V. G. J. Stoks, R. A. M. Klomp, C. P. F. Terheggen, and J. J. de Swart, *Phys. Rev. C* **49**, 2950 (1994).
- [3] R. Machleidt, *Phys. Rev. C* **63**, 024001 (2001).
- [4] R. B. Wiringa, V. G. J. Stoks, and R. Schiavilla, *Phys. Rev. C* **51**, 38 (1995).
- [5] V. G. J. Stoks *et al.*, *Phys. Rev. C* **48**, 792 (1993).
- [6] S. C. Pieper, V. R. Pandharipande, R. B. Wiringa, and J. Carlson, *Phys. Rev. C* **64**, 014001 (2001).
- [7] K. Ermisch *et al.*, *Phys. Rev. C* **68**, 051001(R) (2003).
- [8] K. Ermisch *et al.*, *Phys. Rev. C* **71**, 064004 (2005).
- [9] R. Bieber *et al.*, *Phys. Rev. Lett.* **84**, 606 (2000).
- [10] K. Ermisch *et al.*, *Phys. Rev. Lett.* **86**, 5862 (2001).
- [11] K. Sekiguchi *et al.*, *Phys. Rev. C* **65**, 034003 (2002).
- [12] K. Sekiguchi *et al.*, *Phys. Rev. C* **70**, 014001 (2004).
- [13] N. Sakamoto *et al.*, *Phys. Lett.* **B367**, 60 (1996).
- [14] H. Sakai *et al.*, *Phys. Rev. Lett.* **84**, 5288 (2000).
- [15] S. A. Coon and M. T. Pena, *Phys. Rev. C* **48**, 2559 (1993).
- [16] S. A. Coon *et al.*, *Few-Body Syst.* **30**, 131 (2001).
- [17] A. Deltuva, R. Machleidt, and P. U. Sauer, *Phys. Rev. C* **68**, 024005 (2003).
- [18] B. S. Pudliner, V. R. Pandharipande, J. Carlson, S. C. Pieper, and R. B. Wiringa, *Phys. Rev. C* **56**, 1720 (1997).
- [19] H. Witała, W. Glockle, D. Huber, J. Golak, and H. Kamada, *Phys. Rev. Lett.* **81**, 1183 (1998).
- [20] G. G. Ohlsen, *Rep. Prog. Phys.* **35**, 717 (1972).
- [21] K. Hatanaka *et al.*, *Phys. Rev. C* **66**, 044002 (2002).
- [22] Y. Maeda *et al.*, in *Proceedings of the 17<sup>th</sup> International Conference of Few-Body Problems in Physics (FB17)* (Elsevier, Amsterdam, 2004).
- [23] W. Haeblerli *et al.*, *Phys. Rev. C* **55**, 597 (1997).
- [24] R. V. Cadman *et al.*, *Phys. Rev. Lett.* **86**, 967 (2001).
- [25] B. v. Przewoski *et al.*, *Phys. Rev. C* **74**, 064003 (2006).
- [26] P. F. Bedaque *et al.*, *Annu. Rev. Nucl. Sci.* **52**, 339 (2002).
- [27] E. Epelbaum, *Prog. Part. Nucl. Phys.* **57**, 654 (2006).
- [28] A. M. van den Berg, *Nucl. Instrum. Methods B* **99**, 637 (1995).
- [29] H. J. Wörtche, *Nucl. Phys.* **A687**, 321c (2001).
- [30] R. Bieber *et al.*, *Nucl. Instrum. Methods Phys. Res. A* **457**, 12 (2001).
- [31] H. Mardanpour *et al.*, doi:10.1140/epja/i2006-10228-0.
- [32] V. Hannen *et al.*, *Nucl. Instrum. Methods A* **500**, 68 (2003).
- [33] H. R. Amir-Ahmadi *et al.*, *Nucl. Instrum. Methods A* **562**, 338 (2006).
- [34] H. Witała *et al.*, *Phys. Rev. C* **63**, 024007 (2001).
- [35] A. Deltuva, A. C. Fonseca, and P. U. Sauer, *Phys. Rev. C* **71**, 054005 (2005).